EARTH'S CRYOSPHERE
SCIENTIFIC JOURNAL

Earth's Cryosphere, 2021, vol. XXV, No. 5, pp. 36–46 http://earthcryosphere.ru/

CRYOSPHERE RESEARCH METHODS

THE STUDY OF SEASONAL VERTICAL CHANGES OF GROUND SURFACE IN THE POLAR URAL FOOTHILLS BASED ON FIELD MEASUREMENTS AND ALOS PALSAR RADAR INTERFEROMETRY

V.V. Elsakov, D.A. Kaverin, V.M. Shchanov

Institute of Biology, Komi Science Centre UrB RAS, Kommunisticheskya str. 28, Syktyvkar, 167982, Russia; elsakov@ib.komisc.ru, dkav@mail.ru, shchanov@ib.komisc.ru

Interferometric pairs of ALOS PALSAR dataset (2007–2010) were used to estimate the seasonal and long-term variations in the ground surface height in the piedmont of the Polar Ural, the far northeast of European Russia. The obtained results were validated by ground-truth measurements at the CALM R2 site (active layer thickness monitoring site). The values and amplitude of ground surface height variations obtained from the satellite imagery were lower compared to field measurements. The sites under study were classified in two conditional groups: more drained sites (confined to the upper parts of the moraine ridges) and sites with higher moisture content in the soil (lower parts of the slopes). This classification was based on the intensity of seasonal changes in the height of ground surface during the vegetation period of 2007. Significant correlations between *in situ* and remote sensing-based measurements were established for these groups. The convergence of the results increased with a greater number of *in situ* measurements inside the pixel of the satellite image. The greatest differences in the magnitude of vertical movements of ground surface were reported in the years with contrasting weather conditions (2007 and 2010). Ground surface subsidence was reported to be greater (up to 1.5–4.5 cm) during the colder and wetter vegetation period of 2010, and less pronounced in a drier and warmer season of 2007 (0–3.0 cm) within tundra zones of the Pechora Lowland. A summer heave of ground surface was noted (up to 2–3 cm) in sites with moraine deposits in the piedmont plains for the whole period of observations.

Keywords: *differential radar interferometry, piedmont landscapes of the Polar Ural, ground subsidence and heave.*

INTRODUCTION

Changes in ground surface elevation can be caused by various geological (both exogenous and endogenous) processes [*Dobrovolsky, 2001*]. The differential interferometry synthetic aperture radar (DInSAR) technique is based on analysis of the phase shift of the echo signals of multitemporal images, which allows measuring ground surface displacements to a centimetre-level accuracy over large areas. Interferometry using data from spaceborne SAR instruments has proven to be not inferior to conventional geodetic monitoring methods [*Musikhin, 2012; Chimitdorzhiev et al., 2013*]. Present-day DInSAR-based investigations deal with the analysis of surface-level variations induced by both natural and technogenic effects: underground mine workings [*Epov et al., 2012*], oil extraction [*Evtyushkin, Filatov, 2009; Elsakov, 2012*], and growth of urban areas [*Gorny et al., 2010*].

Cycles of freezing and thawing of the active layer containing different amounts of ground ice are among major causes of vertical movements of the ground surface in permafrost regions [*Kachurin, 1961; Bockheim, 2015*]. Recent years have seen an increased interest in monitoring of natural surface deformations in the permafrost zone considered as indicators of cryogenic landscapes changes at a local or regional level. The balance between multidirectional seasonal thaw subsidence and heave processes is one of the key indicators of changes in permafrost and thermokarst development. The intensity of winter heave and summer subsidence of the ground surface is largely related to climatic conditions [*Mazhitova, Kaverin, 2007; Romanovsky et al., 2008*].

Meteorological observations in the north of Russia demonstrate the existence of a steady warming trend during the period 1976–2012 marked by increased surface air temperature (SAT) [*Leshkevich, 2014*]. This has resulted in a higher rate of permafrost degradation and enhanced biological productivity of tundra plant communities, while the implications of climate change in the Arctic are spatially heterogeneous [*Elsakov, 2017*]. The informative value of DInSAR methods is noted in research of Alaska ecosystems [*Liu et al., 2010*], the Canadian Arctic Archipelago [*Short et al., 2014; Rudy et al., 2018*], Central Siberia [*Chimitdorzhiev et al., 2013; Antonova et al., 2018*], the Tibetan plateau [*Chen et al., 2013*], etc. More frequent surveying (up to 6–12 days for Sentinel-1A/B) has made the method indispensable for

studyes of the seasonal dynamic of the mosaic permafrost landscapes. However, given that interferograms are generated for meteorologically different years and span a relatively short period, they need to be validated by systematic ground-based observations. A lack of available and unified field measurements for verification and calibration of the results obtained has been the biggest constrain to expanding DInSAR-based applications for monitoring the northern areas. This was primarily due to the curtailment of many long-term monitoring programs at permanently operating integrated geocryological and biocenotic research stations in the last decades. The established and subsequently expanded Circumpolar Active Layer Monitoring (CALM) network allow resuming the collection and unification of datasets from long-term observations of changes in seasonal thaw depth (active layer thickness, ALT) and ground surface deformations in permafrost areas [*Brown et al., 2000*].

The aim of this work was to compare seasonal and interannual vertical movements of permafrost-affected soil surface within the piedmont plain of the Polar Urals calculated with interferometric pairs of ALOS PALSAR images and the data of field topographic surveys obtained in the meteorologically contrasting years.

STUDY AREA

The study area is located in the northeast of European Russia in the southern hypoarctic tundra subzone which abuts with the Polar Urals (Fig. 1, *A*) [*Geobotanical zoning..., 1989*]. According to the map of Neogene-Quaternary deposits of Vorkuta district (scale 1:200 000) and the accompanying Explanatory Note [*Shishkin et al., 2013*], three regions are identified within the study area based on its geological structure [*Shishkin et al., 2013*]. The western part is located within the platform plain having a thick sedimentary cover of glacial deposits (up to 40 m) and thinner alluvial-marine deposits (up to 20 m) and includes areas of fens and raised bogs (Fig. 2, *A*). The flat terrain is subsequently replaced to the east by piedmont and intermountain plains with patches of gently undulating outwash plains passing into a hilly glacial plain with areas of accumulative-denudation plain composed of up to 5 m thick lacustrine-glacial deposits. The eastern part of the study area includes a mountain belt whose area is dominated by flat-topped rough and low mountains.

The study area is characterized by continuous and discontinuous permafrost distribution with a thickness of 50–150 m and mean annual ground temperature from 0 to –2 °C [*Ershov, 1996*]. The permafrost table has a complex configuration with through taliks beneath watersheds and river beds. The depth of seasonal thaw of soils is highly differentiated depending on the vegetation cover patterns and snow cover thickness. Shallow (up to 1 m) occurrence of the permafrost table is rather common for moss-dwarf shrub tundra, while permafrost usually occurs at a depth of 1–2 m and more under large-shrub or willow communities [*Mazhitova, 2008*]. Analysis of the vegetation map generated with the supervised classi-

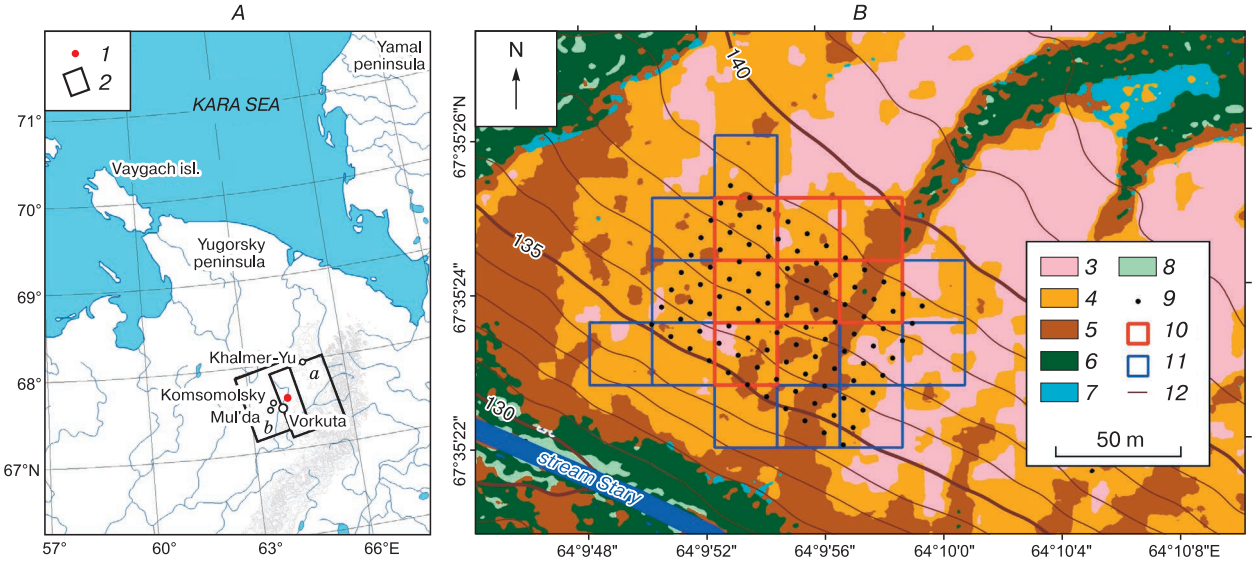

Fig. 1. The location of CALM R2 site and contours ALOS PALSAR dataset (*A*). The distribution of field observation points and PALSAR pixel net (25 × 25 m) within the instrumental measurement site (*B*).

1 – CALM R2 monitoring site; *2* – contours of ALOS PALSAR images; *3* – low-shrub-lichen tundra; *4* – dwarf shrub tundra; *5* – low bush tundra; *6* – willow-shrubs; *7* – swampland complexes; *8* – grass communities; *9* – reference rods for in situ measurements; *10* – pixels assigned in 2007 to the cluster "upper parts of the sloping hill"; *11* – pixels for the cluster "lower parts of the sloping hill"; *12* – contour lines.

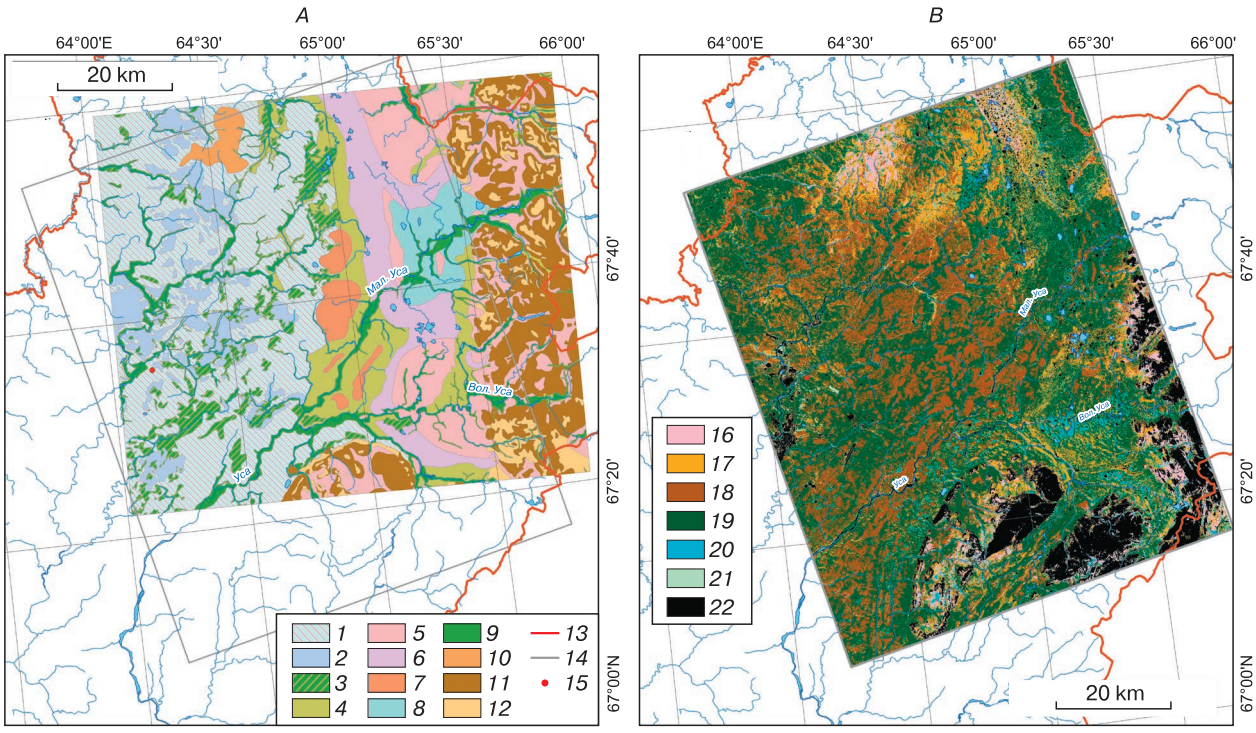

Fig. 2. Main geomorphological elements (*A*) and dominant vegetation cover classes (Landsat 7 ETM+ processing) (*B*).

Landscape-geomorphological complexes: *1–3* – platform plain (*1* – rolling-undulating smoothed glacial plain; *2* – gently undulating plain with alluvial-marine alluvial sediments; *3* – peatlands); *4–10* – piedmont and intermontane plains (*4* – outwash plain; *5* – rolling glacial plain on the Khanmei moraine; *6* – marginal rolling ridge-like glacial debris accumulation formations; *7* – rolling-ridge glacial plain on the Pachvozh moraine; *8* – accumulation-denudation plain on lacustrine-glacial deposits of the Khanmei moraine; *9* – floodplain terraces; *10* – rolling steeply-sloping denudation plain); *11, 12* – mountain belt (*11* – steep glacial-exaration slopes; *12* – gentle slopes with glacial accumulative deposits); *13* – boundaries of the Komi Republic; *14* – ALOS PALSAR satellite image contours; *15* – location of the CALM R2 site. Vegetation cover classes: *16* – low-shrub-lichen tundra; *17* – dwarf shrub tundra; *18* – shrub tundra; *19* – willow shrub; *20* – bog plant association complexes; *21* – grass communities; *22* – barren patches.

fication of Landsat 7 ETM+ imagery (shooting: 137.7.2000) (Fig. 2, *B*) has revealed seven dominant classes of vegetation cover. The tundra plant communities are represented by shrub (20.7 % of the image area), dwarf-shrub (15.6 %) and shrub-lichen (4.7 %) vegetation. Azonal groups include willow shrubs (42.2 %), bog plant species assemblages (5.6 %), areas of grass communities (0.6 %). Territories without vegetation cover account for 10.3 % of the area.

The choice of the study area and the selection of satellite imagery was prompted by the availability of the CALM R2 monitoring site (67°35.04′ N, 64°09.09′ E) located 13 km northeast of Vorkuta city and having long-term series of ALT measurements, surface elevation and soil temperature. The CALM R2 site (81 × 88 m in size) is located on the southwestern slope of a riverine ridge and consists of a network of 99 permanent observational grid nodes with 9 × 8 m grid cells (Fig. 1, *B*). The surface slope is on average 3°, the elevation difference is not more than 4 m. The main orographic elements of the site are flat hilly-ridge uplands with flat slightly convex tops and long gentle slopes [*Druzhinina, Myalo, 1990*]. The vegetation cover of the site is mosaic, dominated by communities of small dwarf-moss tundras on the tops of watershed ridges, large shrub tundras on the slopes of ridges, and bog complexes in depressions and on the flat tops of ridges. The site is dominated by gley soils on clay loams; ice content of the underlying permafrost varies from 40 to 50 % [*Mazhitova, Kaverin, 2007*]. The average ALT varied from 86 to 89 cm during the study period.

RESEARCH METHODS

Monitoring studies. Within the CALM R2 key site year-round soil temperature measurements (at depths of 0, 0.2, and 0.5 m) were carried out using HOBO U-12 data loggers, and ALT was measured with graduated metal probe stick. To determine the heaving/subsidence of the soil surface in all grid nodes of the site, the elevations of the permafrost top and soil surface were measured annually after the

snowmelt (late May) and at the end of the warm season (late September). The measurements were taken with a common instrumental levelling method using Geobox N8-32 optical level with 1.5 mm per 1 km accuracy. A state geodetic survey benchmark located 100 m away from the site served as a stationary reference to determine absolute heights.

The main climatic parameters were derived from the RIHMI–WDC (Russian Institute of Hydrometeorological Information-World Data Center) archive data (*http://www.meteo.ru*). When characterizing the weather conditions at the time of SAR images acquisitions, the weather archive for the weather station in Vorkuta (airport) (WMO ID 23226) (*http://rp5.ru*) was used. To assess the influence of meteorological factors on vertical movements of the ground surface, a sum of average daily positive (thawing degree days, TDD) and negative (freezing degree days, FDD) air temperatures were calculated for the hydrological years (October 1 – September 30) of the study period.

Satellite images processing. Satellite images were processed using the ENVI SARscape module. The phase unwrapping was obtained with the "Minimum Cost Flow" automated algorithm. The parameters of ground control points (*GCPs*) within the runway segments of the Vorkuta airport were taken into account during phase unwrapping. The 2007–2011 ALOS PALSAR images (Fine Beam Dual scanning mode, *L* range, 23.5 cm wavelength, 34.3° off-nadir angle for all scenes) were used to construct two sets of overlapping interferometric pairs (Table 1). In the *L*-range radar imaging, the height of vegetation can be ignored, since the signal is predominantly reflected from the ground surface. Surface deformations were determined by their comparison with master images (15.08.07 and 18.09.07). Master images were selected by the least visual distortion of the resulting interferograms associated with the atmospheric phase delay (caused by atmospheric effects). For most of the compared images, the perpendicular component of the baseline (Bn) had acceptable values (from 298 to 2128 m). The differential interferogram was calculated from the ArcticDEM digital elevation model which was used as a terrain data source (*https://www.pgc.umn.edu/data/arcticdem*).

The surface level displacement was computed for satellite images with 25 m pixel size and the noise was suppressed by applying adaptive filtering before the phase unwrapping. The weather conditions were inferred from information on the shooting time (17:30 UTC) (Table 1). The effect of precipitation and cloud cover on most of the images was negligible. Scenes with signal distortions (i.e. inaccurate phase shift) caused by atmospheric interference were rejected from the analysis.

Table 1. **ALOS PALSAR scenes and weather conditions on the shooting dates**

No.	ALOS PALSAR scenes	Bn, m	N, %	Daily precipitation
Path/Frame 529/1350 17:42 UTC (*a*)				
1	18.09.07 (master-image)		40	–
2	18.06.07	615	100	drizzle, 2.6 mm
3	08.08.09	2128	100	rain
4	26.06.10	1018	70–80	rain shower, 0.2 mm
5	11.08.10	1479	100	drizzle, 7.0 mm
Path/Frame 527/1350 17:35 UTC (*b*)				
6	15.08.07 (master-image)		100	–
7	30.06.07	298	<10	–
8	30.09.07	512	100	light rain shower, 4.4 mm
9	02.07.08	1621	–	–
10	08.07.10	1389	20–30	–
11	23.08.10	1808	70–80	rain shower, 6.0 mm
12	17.08.08	5269	60	rain, 0.1 mm

Note. Bn – perpendicular baseline; N – cloudiness, according to the Vorkuta (airport) weather station archive (WMO ID 23226).

Analysis of temporal variations in the ground surface. Characterization of the seasonal variations in the ground surface movements within the key site was made by two approaches. The first approach analyzes the pairs of PALSAR images from the same set which differ maximally in shooting dates within the season (for summer subsidence: 30.06–30.09.07 and 08.07–23.08.10; for winter frost heave: 30.09.07–02.07.08). The available image pairs often did not represent the maximum values of seasonal subsidence and heave. The comparison of satellite data with in situ measurements made on adjacent dates allows comparing the methods employed.

The second approach is focused on the course of seasonal changes of the ground surface using complete sets of scenes. ALOS PALSAR surveys provide interferometric measurements with the 46-day repeats, thus allowing taking not more than 3–4 images per year during the snow-free period. However, the set of images included two territorially overlapping groups (their boundaries are shown via contours marked as *a* and *b* in Fig. 1). Changes in the soil surface level were computed for all the images from the set of group *a* (master scene 18.09.07) and *b* (master scene 15.08.07). Master images of two groups were not mutually calibrated by soil surface elevation and were acquired on different dates. Therefore, the indicators were recalculated for different groups using similar-time scenes. Most comparable were images of the end of the growing season (18.09.07 for group *a* and 30.09.07 for group *b*). The values for the ground

surface level were taken as equal numbers for the same sites on these dates and sets of images were calibrated relative to the baseline scene (15.08.07).

Analysis of georeferencing of ALOS PALSAR images has demonstrated "sub-pixel accuracy of georeferencing" [*Baranov et al., 2008*]. The satellite image matrix of the CALM R2 monitoring site is formed by 19 pixels (Fig. 1, *B*). The field observations values were averaged by the pixels of satellite images for comparative analysis of the variance between the ALOS PALSAR data and instrumental measurements. The number of field measurements at a pixel varied from 1 to 10. Results of the satellite and *in situ* measurements were used to compare summer subsidence of the ground surface for meteorologically contrasting years 2007 and 2010. Frost heave values were calculated and compared for the hydrological year 2007/08.

RESEARCH RESULTS

Comparison of changes in ground surface elevations estimated from satellite images and instrumental measurements. Comparison of the results of the DInSAR data processing and field measured elevations demonstrated that the values for the ground surface movements over 2007 were distinctly separated into two conventional groups according to their position in the relief (Fig. 3, *a*): drained, predominantly upper parts of the hill (summit, 7 pixels) and lower, essentially wetter (hill base, 12 pixels) areas. When split, the compared indicators obtained by different methods showed significant correlations (for the summit group the rank correlation coefficient $r = 0.83$, probability $p < 0.05$ with total number of observations $n = 7$, for the hill base group: $r = 0.86$, $p < 0.01$, $n = 12$). Significant correlations observed

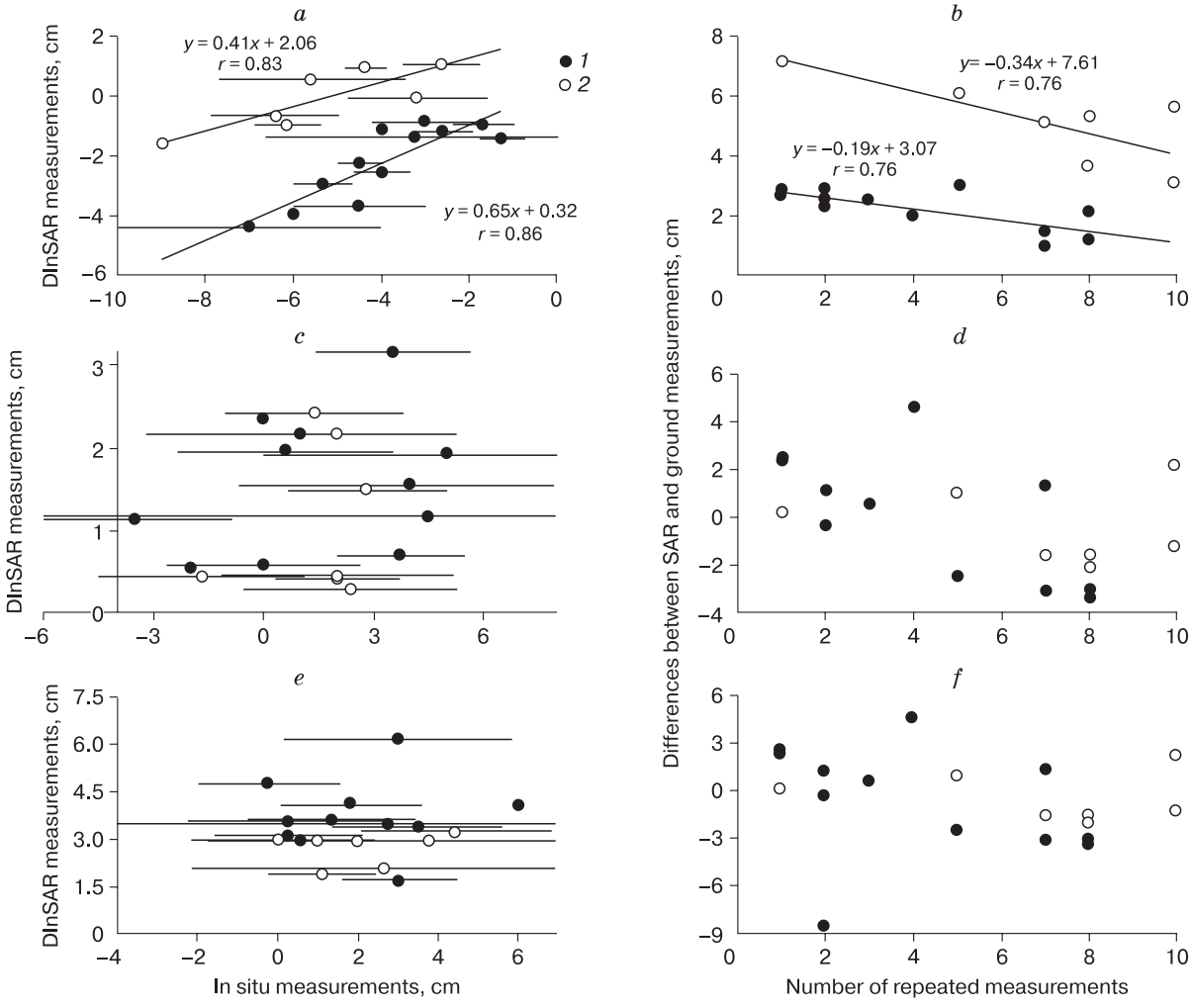

Fig. 3. Seasonal vertical movements of the ground surface from satellite imagery and field measurements.

The mean volumes and standard deviation (SD) are presented (*a*, *c*, *e*). Subsidence is presented by negative value. Measurements dates: *a* – 30.06–30.09.07; *c* – 08.07–23.08.10; *e* – 30.09.07–02.07.08. Differences between the values of satellite and ground methods and numbers of ground measurements (*n*) in pixel of satellite image (*b*, *d*, *f*): *b* – 30.06–30.09.07; *d* – 08.07–23.08.10; *f* – 30.09.07–02.07.08. Groups of pixels assigned to: *1* – lower part of the sloping hill; *2* – upper part of the sloping hill.

between indicators obtained by different methods of measurements allowed separation of the value set into two clusters differing in their location in the relief: for the summit group the rank correlation coefficient (r) 0.83 (n = 7, $p < 0.05$), for the base of hill group 0.86 (n = 12, $p < 0.01$). The difference between the values of satellite and field observations was the slightest for the cluster of pixels located at the lower part of the hill. The satellite measurements had lower values and amplitudes of variations compared to the pointwise in situ measurements. The upper (drained) segments of the hill are characterized by lesser seasonal surface deformations according to the DInSAR data: from the heave of 1.1 cm to subsidence of 1.7 cm. The *in situ* measurements at the sites were marked by a greater magnitude and amplitude of variation: from 2.6 to 9.0 cm of subsidence. The data obtained by the different methods equally demonstrated that surface deformation in the lower parts of the bluff is represented by subsidence only: from 0.8 to 4.4 cm with DInSAR data and from 1.4 to 7.0 cm with *in situ* measurements. A more pronounced soil surface subsidence in the lower part of the site is associated with higher water content and active thawing of ice-rich ALT layers. The differences between ground-based and remote measurements can be explained by different size of the measurement areas: ground measurements are pointwise, while the size of pixels utilized in ALOS PALSAR images covers an area sized 25 × 25 m. The inconsistency between the results obtained by different methods tended to decrease with higher number of measurement points per pixel (r^2 = 0.58, n = 12, $p < 0.01$ and r^2 = 0.59, n = 7, $p < 0.05$) and proved to be minimal (<1.0 cm) for the lower parts of the hill at n = 7–8 (Fig. 3, *b*).

Results showed the largest mismatch (up to 7.3 cm) for the segments in the upper parts of the hill and with single instrumental measurements at the pixel. On average, the mismatch decreased from 0.2 cm (base) to 0.3 cm (summit) per each additional point of *in situ* measurements. The agreement of results obtained by different methods in 2007 was good due to very close dates of DInSAR acquisitions and field observations.

The differences for the 2010 growing season were largely related to shorter intervals for DInSAR observations (only 46 days) by the instrumental method. Low- and medium-amplitude ground surface heave (08.07–23.08.10) was determined from satellite (0.3–3.2 cm) and instrumental (0–5 cm) measurements at the key site. The subsidence of up to 3.5 cm was recorded at several pixels (Fig. 3, *c*). The pixels splitting into clusters according to the relief features was found inconsistent with the year 2007, and the values of in situ measurements showed higher variability. The larger number of measurements at the pixel did not improve the agreement between the satellite and field measurements (Fig. 3, *d*) due to a lesser overlaying of intervals of observations with these methods. The relatively low surface subsidence can be explained by lower summer air temperatures but high amount of precipitation (44 % higher than mean annual) during the 2010 growing season (Table 2). The greater subsidence in the warmer and less the humid year 2007 has demonstrated the permafrost response (depending on local topography and surface conditions) to air temperature warming.

The measured surface heave was 1.7–6.2 cm (DInSAR estimates) and 0–6.0 cm (in situ measurements) at the monitoring site during the 2007/08 winter season. The greatest DInSAR-derived displacements were reported from sites assigned to the cluster of the base of the hill (Fig. 3, *e*). Increasing of number of *in situ* measurements in pixel did not improve convergence.

Seasonal changes in soil surface. The weather conditions are interpreted as the most contrasting during the periods 2006/07 and 2009/10 among the compared periods (Table 2). The diversity of surface air temperature characteristics in different years is reflected in the ALT temperature records. Ground temperatures reached the minimum (–3.7 °C) at a depth of 0.2 m to April 2010 due to a larger amount of winter precipitation and snow isolation. The minimal soil temperature in 2007 was recorded earlier, in the beginning of March (–3.3 °C) due to lower precipitation amount. The daily mean soil temperatures in 2007 were in the range from +0.8 to +2.1 °C (depth:

Table 2. **Climatic indicators for the compared years of observation**

Hydrogeological years	Temperature			Amount of precipitation, mm		
	TDD, °C·days	*FDD*, °C·days	T_{mean}, °C	per year	liquid	solid
2006/07	1277 (14.9)	–2498 (8.9)	–3.8	489	220 (–15.7)	269 (–20.9)
2007/08	1126 (1.4)	–2322 (15.3)	–3.6	525	195 (–25.4)	331 (–2.8)
2008/09	1046 (–5.9)	–2604 (5.0)	–4.5	613	252 (–3.3)	361 (6.2)
2009/10	995 (–10.4)	–3542 (–29.2)	–7.0	776	376 (44.4)	399 (17.4)
Average	1111	–2742	–4.7	600.7	260.6	340.1

Note. The values in parentheses are standard deviations from the multiyear means (%). T_{mean} – mean annual air temperature.

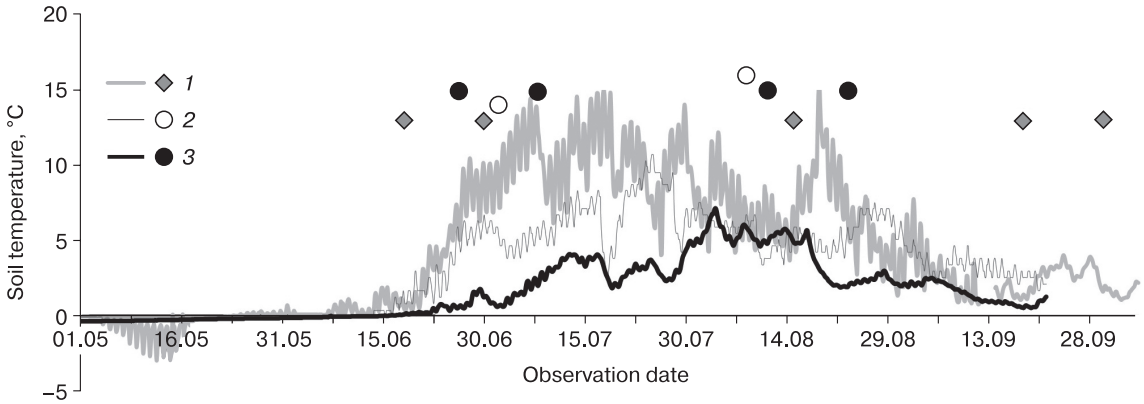

Fig. 4. The soil temperature dynamic at a depth of 0.2 m during growing seasons in different years with the 3 h measuring step.

1 – 2007; *2* – 2008; *3* – 2010.

0.2 m) and from –0.1 to –0.2 °C (depth: 0.5 m) (Fig. 4) at the time of the first survey (18.06.07) because of the early warming of the soil profile. The soil temperatures warmed slowly in the 2010 growing season: transition over 0 °C (TDD) at 0.2 m depth was recorded in mid-June. By the time of the first survey (26.06.10) the ground temperature had warmed to +0.5 ... +0.6 °C.

The 2007 growing season was the warmest within the observation period. Differences in summer air temperatures for growing seasons of different years demonstrate a clearly TDD decreasing trend from 2007 to 2010 (Table 2). Soil was warming most intensely in the first half of the summer 2007 and the maximum temperature (+14.3 °C) at a depth of 0.2 m was recorded on July 6 (i.e. 6 days after the PALSAR acquisitions). Soils demonstrated slower heating in 2010: maximal temperature (+7.1 °C) was recorded on August 3.

The average ALT depth was close for years with contrasting temperature conditions: (89 ± 14) cm in 2007 and (89 ± 13) cm in 2010 (n = 99). The summers in these years were characterized by remarkable differences in the surface air temperatures (SAT) effected the ground which were balanced by contrasting summer rainfall amount. Results of ground deformation measured *in situ* showed a subsidence of surface (4.0 ± 3.5) cm (n = 19) at the CALM site during May–September 2007, against its heave (2.2 ± 4.9) cm noted in 2010. The 2008 temperature values occupied an intermediate position between 2007 and 2010. First PALSAR acquisitions of 2007 and 2010 were coincident with the beginning of soil heating (freeze-thaw transition), which suggests a minimal partial compensation for winter heave. The exception is 2008, when first acquisitions were coincident with the heating of compared soil depth (0.2 m) to 5 °C.

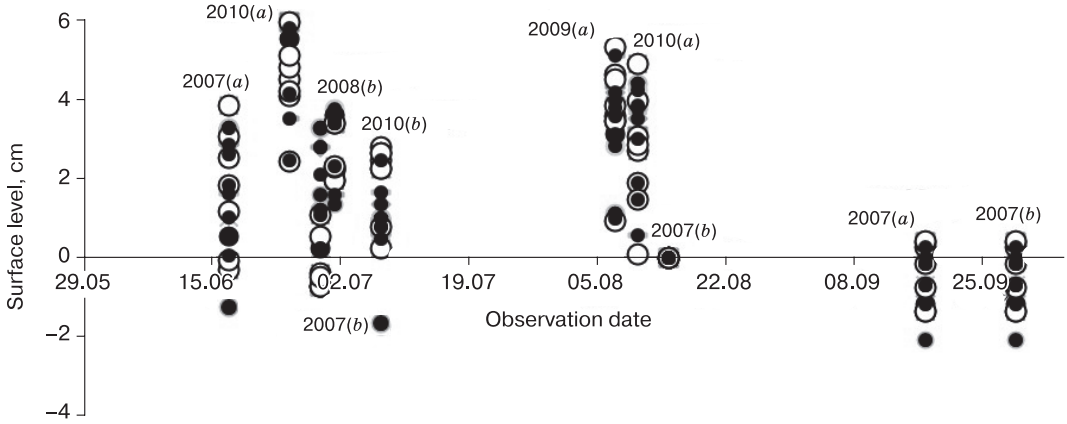

Fig. 5. Ground vertical movements at the CALM R2 monitoring site for different years.

Satellite image pairs: *a* – 529/1350; *b* – 527/1350; parts of the lower part of the slope hill (dark dots) and upper part (light dots). The zero value of surface level is taken for date of master-image (15.08.07).

The ground surface dynamics for growing seasons of different years based on remote sensing method was determined from comparison of the subsidence/heave amplitudes within the monitoring site pixels on satellite images. The maximum soil surface subsidence within the observation period was reported in 2007 (Fig. 5), similarly to the *in situ* measurements. The average variation in ground surface elevation in the upper part of the hill was characterized by lower values (subsidence: 0 to 1 cm) against its base (2 to 4 cm) in that year. The disagreement in estimates for seasonal variations on the 2010 scenes (reduction from 26.06.10 to 08.07.10 with subsequent increase by 11.08.10) was most likely to be a result of using different sets of satellite scenes (527/1350 and 529/1350).

In terms of magnitude of land-surface subsidence, the weather conditions of the 2009 summer season were the most consistent with the years 2010, and 2007 with 2008, which is also corroborated by soil temperatures and meteorological parameters, accordingly (Table 2). The winter seasonal heave was only slightly compensated by summer subsidence during the years with relatively cold summers (2009 and especially 2010).

The seasonal and interannual vertical surface movements at a regional level. Satellite imagery offering a good spatial coverage (the ALOS PALSAR scene size covers an area of 69 × 87 km) allows detecting and quantifying vertical ground surface movements within large areas. The maximal vertical surface displacements noted on human-affected areas (e.g., recent backfill or soil removal and subsidence in coal-mining areas).

The summer surface subsidence of undisturbed soil cover is fragmentarily presented (Fig. 6, *A*) at the mining field of the coal-mining company Vorkutaugol. It was rather considerable in amplitude (>16 cm), but area was small (0.7–1.0 km diameter) in different years. Localities of subsidence sites varied from year to year (Fig. 6, *B*). The 2012 field studies revealed no visible changes in the moss-lichen cover and structure of plant communities at these sites.

Significant seasonal ground displacements are not inherent to the undisturbed tundra ecosystems (Fig. 7). The largest areas where summer settlement of the soil surface (up to 3 cm) is observed on natural depressions of drainage hollows and downgraded areas between hills. Low (1.5–3.0 cm) and moderate amplitudes (3.0–4.5 cm) of surface subsidence were observed on 30–40 % of the area of swampland ecosystems and large-shrub tundra in the summer of 2007 and 2010. Low heaves of soil surface were reported within 23 % of the area of low-shrub lichen tundra. The dwarf birch (*Betula nana*) moss tundra and grass communities showed no significant changes.

The regional soil surface dynamics has been remarkably affected by quaternary sediments distribution (Fig. 2, *A*). The ground surface subsidence was maximal in 2010 (1.5–4.5 cm) and less expressed in 2007 in the flat portion of the study area (Fig. 7). The summer surface heaves (1.5–4.5 cm) were noted at rather large areas in the piedmont plains of the Polar

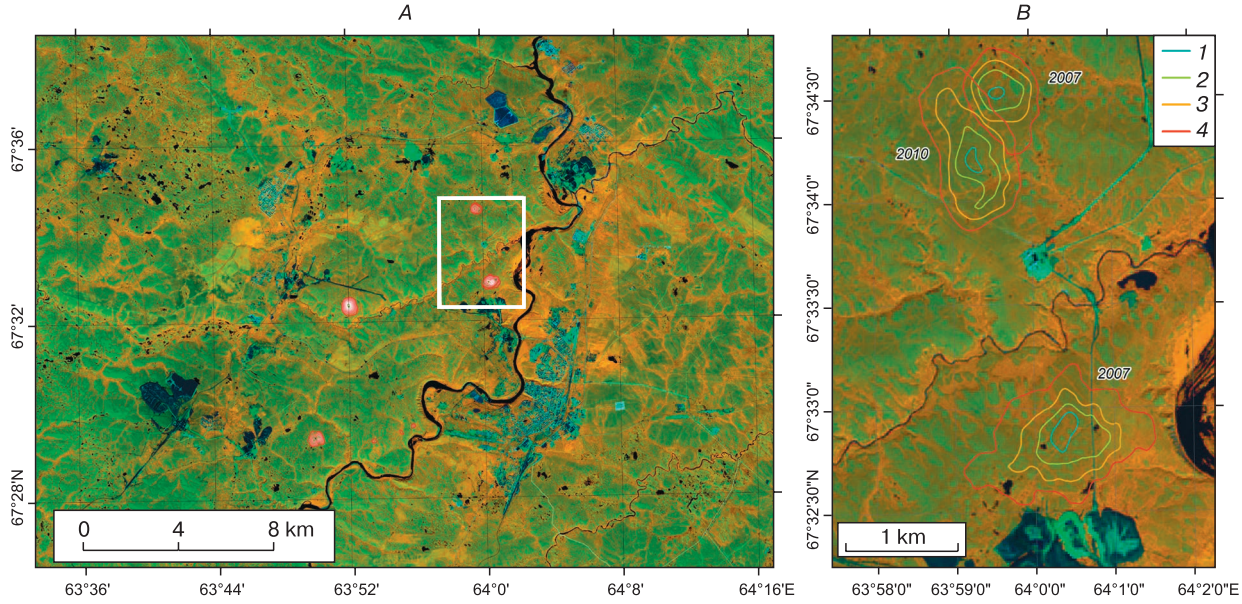

Fig. 6. Subsidences near coal-mines in the vicinity of Vorkuta city in 2007 (*A*) and 2010 (*B*). The colored contour lines mark subsidences.

1 – over 16 cm; *2* – over 12 cm; *3* – over 8 cm; *4* – over 4 cm. Background: Sentinel-2 image acquired 25.07.19 (*http://www.glovis.usgs.gov*).

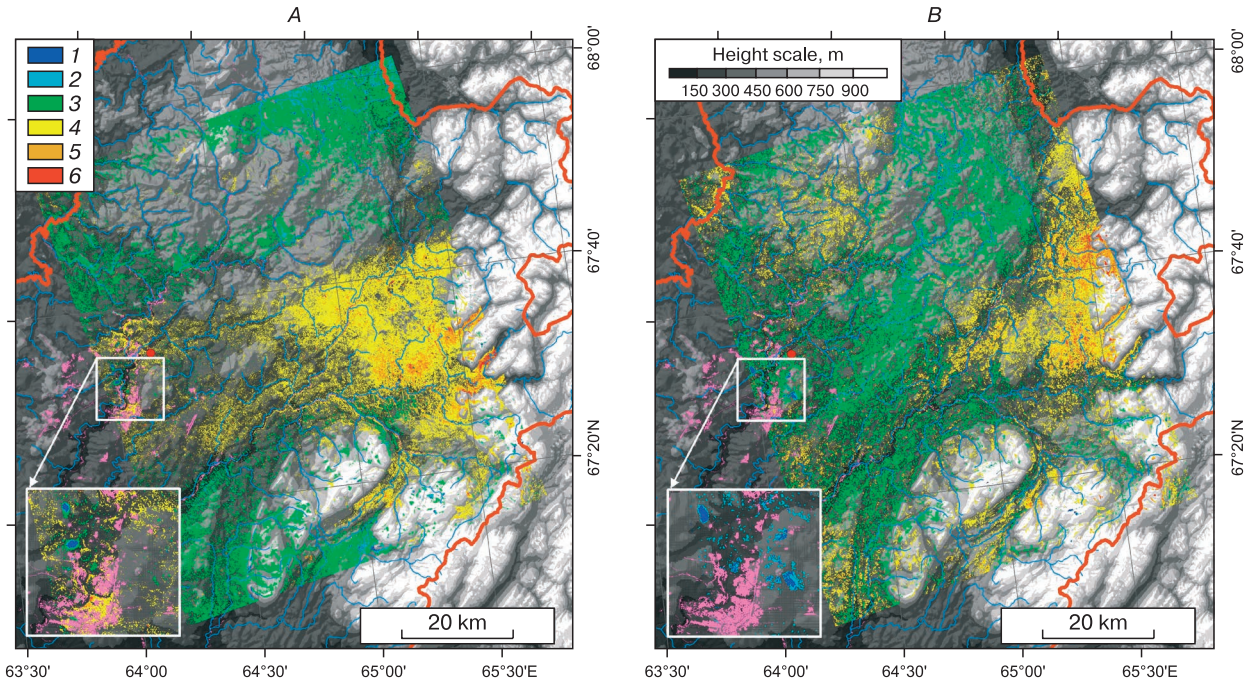

Fig. 7. The ground surface movements on the western slopes of the Polar Urals and Bolshezemelskaya tundra for the periods 15.08–30.09.07 (*A*) and 08.07–23.08.10 (*B*) processed from the ALOS PALSAR data.

Colored areas represent movements of the ground surface: *1* – over –4.5 cm; *2* – from –4.5 to –3.0 cm; *3* – from –3.0 to –1.5 cm; *4* – from 1.5 to 3.0 cm; *5* – from 3.0 to 4.5 cm; *6* – over 4.5 cm. Minor changes (from –1.5 to –1.5 cm) are not highlighted in color. Negative values correspond to the ground surface subsidence. SRTM 90 is the background DEM. The inset shows disturbed areas in the vicinity of Vorkuta city (building plots and areas with disturbed vegetation), colored in pink. The values of local subsidence in the coal-mining areas (blue spots) accord with the legend.

Urals (watersheds of the Bolshaya Usa and Malaya Usa rivers). These sites are located on younger glacial moraine complexes of the Late Pleistocene (Khanmei) glaciation [*Astakhov et al., 2007; Astakhov, 2011*]. The ground surface heave is visible most clearly on the 2010 images.

DISCUSSION

The DInSAR interferometry-derived seasonal vertical movements of the ground surface at the CALM R2 site and the adjacent area are represented by estimates similar to other parts of the Arctic. The subsidence of up to 2 cm was marked within 40 % of the tundra ecosystems in the Lena River delta with TerraSAR-X satellite for 2013–2014 [*Antonova et al., 2018*]. The average values ranged from (1.7 ± 1.5) cm for the relatively cold 2013 to (4.8 ± 2.0) cm for the warm 2014. The magnitude of ground surface deformation measured with ERS 1/2 satellites for Alaska ecosystems (North Slope) ranged in 1–4 cm interval for summer periods of 1992–2000 [*Liu et al., 2010*].

The amplitudes of soil surface displacement in the summer season were largely controlled by sediment composition, variations in ground ice content and sedimentary cover thickness according to the measurements of satellite RADARSAT-2 of ecosystems of the Canadian Arctic Archipelago (Baffin Land) [*Short et al., 2014*]. The minimum displacement (±1 cm) was observed for bedrock outcrops and boulder clays [*Rudy et al., 2018*]. The subsidence of sites with shallow bedrock occurrence demonstrated lower values despite the maximum subsidence features of adjacent areas for warmer summers. The seasonal and interannual low amplitude vertical surface movements with opposite directions were observed in northern Alaska during 1962–2015 [*Streletskiy et al., 2016*].

Soil surface subsidence in the plain part of the study region at summertime is probably associated with the permafrost thaw. Surface subsidence of large magnitude was observed even in relatively cold years (2010) against the backdrop of higher precipitation.

Ground surface heave is not typical during the summer period, but occasionally was reported for the western foothills of the Polar Urals. This may be explained by increasing amount of summer liquid precipitation [*Taskaev, 1997*] in the area dominated by loamy gley soils [*Shishov, 2000*] which are prone to swelling. The heave motion of land-surface in the piedmont landscapes may have been also affected by ground water redistribution, slope processes, seasonal

ice aggradation at the end of vegetation period[1] [*Rudy et al., 2018*] or a systematic error stemming from the DInSAR results calibration [*Antonova et al., 2018*]. About 10–13 % of the alpine tundra of the south part of Melville Island (Canada) demonstrated heave of a ground surface (3.0–4.0 cm) in summers 2013 and 2015 according to the DInSar measurements [*Rudy et al., 2018*].

The highly mosaic tundra soil-vegetation cover hampers comparability of pointwise *in situ* and DInSAR measurements and obstructs for convergence assessment between them [*Short et al., 2011*]. However, verification of DInSAR estimates by *in situ* data is a part of the accuracy assessment procedure. The increased number of instrumental measurements per observation site has contributed to improvement to the results agreement.

The highest agreement between the data was achieved for 2007 at the lower part of the hill with 7–8 instrumental measurements taken within one pixel.

CONCLUSIONS

A good agreement between the results of seasonal and interannual variability in ground surface displacements obtained by *in situ* and DInSAR measurements illustrate the effectiveness of the approach combining both field (instrumental) measurements and satellite observations to the studied permafrost-affected ecosystems. It is possible to reduce disagreement between the results obtained by different methods by larger amount of the *in situ* measurements within the same observation time intervals. To improve the accuracy of displacement estimates with remote satellite data, we need to increase the number of SAR images covering all observation periods.

The DInSAR methods allowed us to divide the CALM R2 monitoring site into two sectors (lower and upper parts of the sloping hill), thereby revealing differences in the ground surface elevation dynamics. Results of satellite and instrumental measurements were minimal in the lower part of the slope.

The opposite movements of soil surface during the summer season identified by the DInSAR method can be caused by landscape differences in the study region. Summer subsidence of ground surface (1.5–4.5 cm) was noted in plain tundra in loamy permafrost-affected soils. The ground surface heave (up to 2–3 cm) noted in the piedmont Polar Urals is associated with excess soil moisture in loamy gley soils in the context of enhanced summer precipitation and slope sediment redistribution. The specificity of weather conditions directly affects the ground surface movement in certain years. The amplitude of ground surface subsidence in summer is generally lower in relatively warm and dry years and higher in cold and wet years.

Satellite imagery allows analyzing ground surface movements on a regional level due to large spatial coverage. By increasing the time coverage of imagery, we can better capture seasonal surface movements and minimize errors in their estimations. A time series of ground surface movements with account of meteorological and landscape parameters can be obtained even for remote and hard-to-reach areas. DInSAR is an actual data source for generating large-scale maps of the ground surface dynamics in permafrost regions.

Acknowledgements. *The research was conducted under the state task to the Institute of Biology of Komi Science Center of Ural Branch of the Russian Academy of Sciences "Revealing general patterns of formation and functioning of peat soils in the Arctic and Subarctic sectors of the European northeast of Russia" (grant AAAA-A17-117122290011-5) and the Circumpolar Active Layer Monitoring (CALM) program. ALOS PALSAR images were obtained under the JAXA RA-6 program (PI 3018).*

References

Antonova, S., Sudhaus, H., Strozzi, T., et al., 2018. Thaw subsidence of a yedoma landscape in Northern Siberia, measured *in situ* and estimated from TerraSAR-X interferometry. Remote Sensing 10 (4), No. 494, 1–27.

Astakhov, V.I., 2011. The cover formation of the final Pleistocene in the far northeast of European Russia. Regional Geology and Metallogeny, No. 47, 12–27.

Astakhov, V.I., Mangerud, Ya., Svendsen, J.I., 2007. Trans-Uralian correlation of the northern Upper Pleistocene. Regional Geology and Metallogeny, No. 30–31, 190–206.

Baranov, Yu.B., Kiselevskii, E.V., Kantimirov, Yu.I., et al., 2008. DEM Building based on the data derived due to the interferometric processing of ALOS PALSAR radar images. Geomatics, No. 1, 37–45.

Bockheim, J., 2015. Cryopedology. Springer, Cham, New York, 177 pp.

Brown, J., Hinkel, K.M., Nelson, F.E., 2000. The circumpolar active layer monitoring (CALM) program: research designs and initial results. Polar Geography 24 (3), 165–258.

Chen, F., Lin, H., Zhou, W., et al., 2013. Surface deformation detected by ALOS PALSAR small baseline SAR interferometry over permafrost environment of Beiluhe section, Tibet Plateau, China. Remote Sensing of Environment 138, 10–18.

Chimitdorzhiev, T.N., Dagurov, P.N., Zakharov, A.I., et al., 2013. Estimation of seasonal deformations of marshy soil by radar interferometry and geodetic leveling techniques. Kriosfera Zemli [Earth's Cryosphere], XVII (1), 80–87.

Dobrovol'sky, V.V., 2001. Geology. VLADOS, Moscow, 320 pp. (in Russian).

[1] Aggradation of ice does not occur late in the growing season. The mechanism for ice aggradation discussed in [*Rudy et al., 2018*] is regarded as being a special case of a thaw slump, and is therefore possible only under extremely cold conditions (ground temperatures below –10 °C). – ***Ed. note.***

Druzhinina, O.A., Myalo, E.G., 1990. Protection of Vegetation of the Far North: Problems and Prospects. Agropromizdat, Moscow, 176 pp. (in Russian).

Elsakov, V.V., 2012. Satellite remote sensing in the environmental monitoring of hydrocarbon production regions. Current Problems in Remote sensing of the Earth from Space, 9 (5), 133–139.

Elsakov, V.V., 2017. Spatial and interannual heterogeneity of changes in the vegetation cover of Eurasian tundra: Analysis of 2000–2016 MODIS data. Current Problems in Remote Sensing of the Earth from Space, 14 (6), 56–72.

Epov, M.I., Mironov, V.L., Chimitdorzhiev, T.N., et al., 2012. Observations of Earth's surface subsidence in the area of Kuzbass underground mines based on ALOS PALSAR radar interferometry data. Earth Observation and Remote Sensing, No. 4, 26–29.

Ershov, E.D. (Ed.), 1996. Geocryological Map of the USSR, scale 1: 2 500 000. Gos. kartogr. fabrika, Vinnitsa, 16 pp. (in Russian).

Evtyushkin, A.V., Filatov, A.V., 2009. Estimation of Earth surface displacements in area of intensive oil production in Western Siberia by SAR interferometry using ENVISAT\ ASAR and ALOS\PALSAR data. Current Problems in Remote Sensing of the Earth from Space, 2 (6), 46–53.

Geobotanical Zoning of the Non-Chernozem Zone of the European Part of the RSFSR, 1989. Nauka, Leningrad, 64 pp. (in Russian).

Gorny, V.I., Kritsuk, S.G., Latypov, I.Sh., et al., 2010. Vertical sign-variable movements of ground surface according to satellite remote sensing data (on an example of Saint-Petersburg). Current Problems in Remote Sensing of the Earth from Space, 7 (2), 231–332.

Kachurin, S.P., 1961. Thermokarst on USSR territory. Izd. AN SSSR, Moscow, 291 pp. (in Russian).

Leshkevich, T.V. (Ed.), 2014. The Second Roshydromet Assessment Report on Climate Change and its Consequences in the Russian Federation. Rosgidromet, Moscow, 1009 pp. (in Russian).

Liu, L., Tingjun, Zhang, T., Wahr, J., 2010. InSAR measurements of surface deformation over permafrost on the North Slope of Alaska. J. Geophys. Res. 115, 1–14.

Mazhitova, G.G., 2008. Soil temperature regimes in the discontinuous permafrost zone in the East European Russian Arctic. Eurasian Soil Science, No. 1, 48–62.

Mazhitova, G.G., Kaverin, D.A., 2007. Thaw depth dynamics and soil surface subsidence at a Circumpolar Active Layer Monitoring (CALM) site, the European North of Russia. Kriosfera Zemli [Earth's Cryosphere], XI (4), 20–30.

Musikhin, V.V., 2012. The interferometric SAR data processing-based monitoring of ground surface subsidence in areas under extensive mineral mining. Extended abstract of Cand. Sci. (Eng.) Dissertation. Perm, 22 pp. (in Russian).

Romanovsky, V.E., Marchenko, S.S., Daanen, R.P., 2008. Soil climate and frost heave along the permafrost / Ecological North American Arctic Transect. In: Proc. of the Ninth International Conference on Permafrost (Fairbanks, Alaska, 28 June–3 July 2008). Institute of Northern Engineering, Univ. Alaska Fairbanks, Fairbanks, vol. 2, pp. 1519–1524.

Rudy, A.C., Lamoureux, S.F., Treitz, P., et al., 2018. Seasonal and multi-year surface displacements measured by DInSAR in a High Arctic permafrost environment. Intern. J. Appl. Earth Obs. Geoinformation 64, 51–61.

Shishkin, M.A., Malykh, O.N., Popov, P.E., Kolesnik, L.S., 2013. The State Geological Map of the Russian Federation, scale 1:200 000, Sheets: Q-41-V, VI (2nd ed.). VSEGEI, Moscow, 262 pp. (in Russian).

Shishov, L.L. (Ed.), 2000. The State Soil Map of Russia, scale 1:1 000 000, Sheet: Q-41 Vorkuta]. FSGKR, Moscow (in Russian).

Short, N., Brisco, B., Couture, N., et al., 2011. A comparison of TerraSAR-X, RADARSAT-2 and ALOS-PALSAR interferometry for monitoring permafrost environments, case study from Herschel Island, Canada. Remote Sensing of Environment, 115, 3491–3506.

Short, N., LeBlanc, A.-M., Wendy, S.W., et al., 2014. RADARSAT-2 D-InSAR for ground displacement in permafrost terrain, validation from Iqaluit Airport, Baffin Island, Canada. Remote Sensing of Environment, 141, 40–51.

Streletskiy, D.A., Shiklomanov, N., Jonathon, D., et al., 2016. Thaw subsidence in undisturbed tundra landscapes, Barrow, Alaska, 1962–2015. Permafrost and Periglacial Processes 28 (3), 566–572.

Taskaev, A.I. (Ed.), 1997. Climate and Hydrology Atlas of the Komi Republic. Dik, Moscow, 115 pp. (in Russian).

URL: http:// www.glovis.usgs.gov (last visited: 18.04.2018).

URL: http://rp5.ru/Архив_погоды_в_Воркута_(аэропорт) (last visited: 18.04.2018).

URL: http://www.meteo.ru (last visited: 30.08.2019).

URL: https://www.pgc.umn.edu/data/arcticdem (last visited: 10.02.2020).

Received December 4, 2018
Revised August 22, 2019
Accepted May 28, 2021

Translated by N.N. Mzhelskaya